

A01-29261

AIAA-2001-2004

AERODYNAMIC INTERACTIONS INVOLVING MULTIPLE PARACHUTE CANOPIES

Keith Stein[†] Richard Benney[‡]
*U.S. Army Soldier and Biological Chemical Command
Soldier Systems Center - Natick, MA 01760, USA*

Tayfun Tezduyar[§] Vinod Kumar[¶] Sunil Sathe^{*}
*Mechanical Engineering and Materials Science
Rice University, Houston, TX 77005, USA*

Eric Thornburg^{**} Clifton Kyle^{**}
*U.S. Military Academy
West Point, NY 10996, USA*

and

Tomoyasu Nonoshita
*Mechanical Engineering
Sophia University, Tokyo, JAPAN*

ABSTRACT

Simulation of airdrop systems using multiple parachutes or parachute clusters may involve the aerodynamic interactions between parachute canopies. These interactions can occur between two separate parachutes when one of them comes close to the other. They also occur between the canopies of a cluster of parachutes. We present results for the interactions involving two separate round parachutes in close proximity to one another, and study the effect of the separation distance on the aerodynamic interaction. We also present results for the aerodynamic interactions between the canopies in a cluster of parachutes, where we study the effect of varying the number and arrangement of the canopies.

* This paper is declared a work of the U.S. Government and is not subject to copyright protection in the United States.

[†] Aerospace Engineer, Corresponding Author

[‡] Aerospace Engineer, Senior Member

[§] James F. Barbour Professor and Chairman

[¶] Graduate Student, Student Member

^{*} Graduate Student

^{**} Undergraduate Student

INTRODUCTION

For some airdrop systems, and under special scenarios, the behavior of a parachute is influenced by its interaction with another parachute (or multiple parachutes). In this paper we describe a modeling approach and present results for simulations involving the aerodynamic interaction between multiple parachutes. Here, the interaction is assumed to be purely aerodynamic, with fluid-structure interactions playing no role. We focus on two different types of interactions. First, we focus on the interaction between two separate parachutes that interact when coming within close proximity of one another. Results from simulations for different separations between the two parachutes are presented. Secondly, we focus on the aerodynamic interaction between multiple parachute canopies in a cluster of parachutes. Interactions for three, four, five, and six parachutes in a cluster are studied. These simulations provide initial results on the aerodynamic interactions for multiple parachutes, but they also serve to demonstrate the utility of these modeling tools for application in airdrop applications.

Follow-on studies will take into account the coupled fluid and structural behavior that occur in these

interactions. Fluid-structure interactions (FSI) are involved at all stages of airdrop systems performance, from initial deployment until landing. The interaction between the parachute system and the surrounding flow field is dominant in most parachute operations, and thus the ability to predict parachute FSI is recognized as an important challenge within the parachute research community.¹⁻⁵

MODELING APPROACH

For the problems presented in this paper, we assume that the parachutes are operating at sufficiently low speeds, and, therefore, the aerodynamics are governed by the Navier-Stokes equations of incompressible flows. Also, we limit our focus to the aerodynamic interaction between the parachute canopies and payloads. For these cases, the canopies experience no shape changes or relative motions and, therefore, the numerical solutions for the fluid dynamics are obtained using a stabilized semi-discrete finite element formulation.⁶ These methods have been implemented for parallel computing using the MPI programming environment. The results presented here are for simulations carried out on a CRAY T3E-1200 supercomputer.

Equations for Incompressible Flows

Let $\Omega_t \subset \mathbb{R}^{n+d}$ be the spatial fluid mechanics domain with boundary Γ_t at time $t \in (0, T)$, where the subscript t indicates the time-dependence of the spatial domain and its boundary. The Navier-Stokes equations of incompressible flows can be written on Ω_t and $\forall t \in (0, T)$ as

$$\rho \left(\frac{\partial \mathbf{u}}{\partial t} + \mathbf{u} \cdot \nabla \mathbf{u} - \mathbf{f} \right) - \nabla \cdot \boldsymbol{\sigma} = 0, \quad (1)$$

$$\nabla \cdot \mathbf{u} = 0, \quad (2)$$

where ρ , \mathbf{u} and \mathbf{f} are the density, velocity and the external force, respectively. The stress tensor $\boldsymbol{\sigma}$ is defined as

$$\boldsymbol{\sigma}(p, \mathbf{u}) = -p\mathbf{I} + 2\mu\boldsymbol{\varepsilon}(\mathbf{u}). \quad (3)$$

Here p , \mathbf{I} and μ are the pressure, identity tensor and the viscosity, respectively. The strain rate tensor $\boldsymbol{\varepsilon}(\mathbf{u})$ is defined as

$$\boldsymbol{\varepsilon}(\mathbf{u}) = \frac{1}{2}((\nabla \mathbf{u}) + (\nabla \mathbf{u})^T). \quad (4)$$

Both Dirichlet- and Neumann-type boundary conditions are accounted for:

$$\begin{aligned} \mathbf{u} &= \mathbf{g} \text{ on } (\Gamma_t)_g, \\ \mathbf{n} \cdot \boldsymbol{\sigma} &= \mathbf{h} \text{ on } (\Gamma_t)_h. \end{aligned} \quad (5)$$

Here $(\Gamma_t)_g$ and $(\Gamma_t)_h$ are complementary subsets of the boundary Γ_t , \mathbf{n} is the unit normal vector at the boundary, and \mathbf{g} and \mathbf{h} are given functions. A divergence-free velocity field is specified as the initial condition.

Finite Element Formulation

Let us consider a fixed spatial domain Ω and its boundary Γ , where subscript t is dropped from both Ω_t and Γ_t . The domain Ω is discretized into subdomains Ω^e , $e = 1, 2, \dots, n_{el}$, where n_{el} is the number of elements. For this discretization, the finite element trial function spaces \mathcal{S}_u^h for velocity and \mathcal{S}_p^h for pressure, and the corresponding test function spaces \mathcal{V}_u^h and \mathcal{V}_p^h are defined as follows:

$$\mathcal{S}_u^h = \{\mathbf{u}^h | \mathbf{u}^h \in [H^{1h}(\Omega)]^{n+d}, \mathbf{u}^h \doteq \mathbf{g}^h \text{ on } \Gamma_g\}, \quad (6)$$

$$\mathcal{V}_u^h = \{\mathbf{w}^h | \mathbf{w}^h \in [H^{1h}(\Omega)]^{n+d}, \mathbf{w}^h \doteq \mathbf{0} \text{ on } \Gamma_g\}, \quad (7)$$

$$\mathcal{S}_p^h = \mathcal{V}_p^h = \{q^h | q^h \in H^{1h}(\Omega)\}. \quad (8)$$

Here $H^{1h}(\Omega)$ is the finite-dimensional function space over Ω . The stabilized finite element formulation is written as follows: find $\mathbf{u}^h \in \mathcal{S}_u^h$ and $p^h \in \mathcal{S}_p^h$ such that $\forall \mathbf{w}^h \in \mathcal{V}_u^h$ and $q^h \in \mathcal{V}_p^h$:

$$\begin{aligned} & \int_{\Omega} \mathbf{w}^h \cdot \rho \left(\frac{\partial \mathbf{u}^h}{\partial t} + \mathbf{u}^h \cdot \nabla \mathbf{u}^h - \mathbf{f}^h \right) d\Omega \\ & + \int_{\Omega} \boldsymbol{\varepsilon}(\mathbf{w}^h) : \boldsymbol{\sigma}(p^h, \mathbf{u}^h) d\Omega \\ & - \int_{\Gamma_h} \mathbf{w}^h \cdot \mathbf{h}^h d\Gamma \\ & + \int_{\Omega} q^h \nabla \cdot \mathbf{u}^h d\Omega \\ & + \sum_{e=1}^{n_{el}} \int_{\Omega^e} \frac{1}{\rho} [\tau_{\text{SUPG}} \rho \mathbf{u}^h \cdot \nabla \mathbf{w}^h + \tau_{\text{PSPG}} \nabla q^h] \cdot \\ & \left[\rho \left(\frac{\partial \mathbf{u}^h}{\partial t} + \mathbf{u}^h \cdot \nabla \mathbf{u}^h \right) - \nabla \cdot \boldsymbol{\sigma}(p^h, \mathbf{u}^h) - \rho \mathbf{f}^h \right] d\Omega \\ & + \sum_{e=1}^{n_{el}} \int_{\Omega^e} \tau_{\text{LSIC}} \nabla \cdot \mathbf{w}^h \rho \nabla \cdot \mathbf{u}^h d\Omega \\ & = 0. \end{aligned} \quad (9)$$

In this formulation, τ_{SUPG} , τ_{PSPG} and τ_{LSIC} are the stabilization parameters.^{6,7}

NUMERICAL EXAMPLES

For all simulations we use tetrahedral meshes. The parachute canopy surface is representative of a C-9 parachute. For the first example, the parachute in the numerical model consists of the canopy and a paratrooper. In the second example, the cluster of parachutes consist of multiple C-9 canopies. Figure 1 shows, for one of the cases, the interior surfaces and a cutting plane through the mesh (left), the parachute canopy surface mesh (center), and the paratrooper (right). The simulations are carried out at a Reynolds number (based on the canopy diameter) of approximately 5 million.

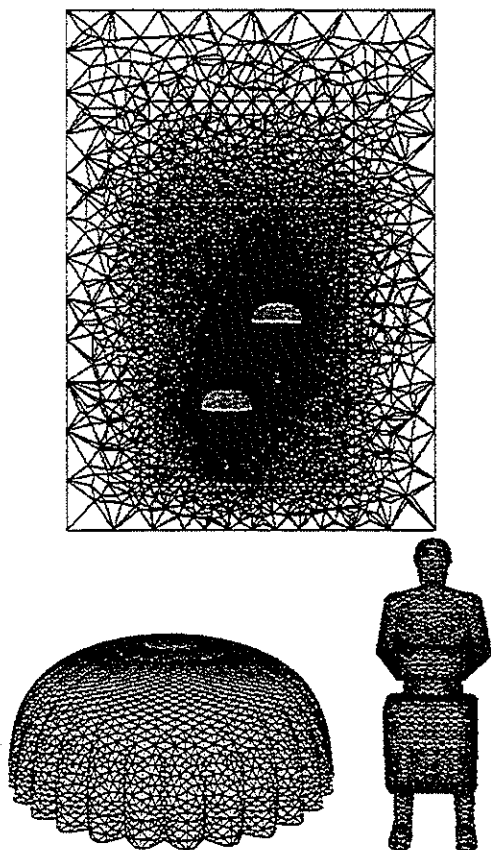


Figure 1. CFD mesh: Cutting plane and interior boundaries (top); Parachute canopy (bottom left); Paratrooper (bottom right).

Interaction Between Two Parachutes

A series of simulations are carried out for the interaction between two separate parachutes (i.e., round canopy and "paratrooper") with horizontal

spacings along the x -axis ranging from zero (i.e., axially aligned) to five inflated parachute radii. Vertical spacings are held at a constant value of approximately one meter between the apex of the lower canopy and the feet of the paratrooper. The parachute model is representative of a 28-foot diameter and 28-gore C-9 personnel parachute. Representation of the geometry for the canopy comes from a separate structural dynamics simulation with a prescribed pressure distribution. Surface representations for the paratrooper and for other boundaries in the CFD model are obtained using a variety of in-house modeling tools, and separate unstructured volume meshes are generated for each case studied. For each of the examples, the two paratrooper and canopy systems are identical, with 8,288 triangular faces describing both the upper and lower canopy surfaces, and 11,714 triangular faces representing the paratrooper. The size of the volume meshes vary from case to case, with approximately 1.8 million tetrahedral elements and 300,000 nodes and resulting in approximately 1.2 million coupled equations for the case with a horizontal spacing of 0.5 radii. In each of the meshes, the mesh refinement is controlled surrounding the paratroopers, canopies, and the wake and interaction regions in order to have a greater concentration of elements in these regions. Descent velocities of 22 ft/s are represented by imposing the following boundary conditions: a uniform upstream boundary condition on the lower boundary, no-slip conditions on the paratrooper and canopy surfaces, zero normal velocity and zero shear stress conditions at the side boundaries, and a traction-free condition at the outflow boundary.

The simulations predict a strong interaction between the upper and lower parachute wakes for spacings of 1 radius and less. In these cases, the upper canopy "loses its wind" and experiences negative drag, upon which the canopy would risk collapsing. The flow fields for horizontal spacings of 0.5, 2.0, and 5.0 radii are shown in Figure 4, with the velocity vectors on the left and the vorticity on the right. This figure indicates a strong interaction between the upper canopy and the lower wake for a horizontal spacing of 0.5 radii, with the upper canopy clearly caught in the wake of the lower canopy. In contrast, very little interaction is seen between the two parachute flow fields for a spacing of 5.0 radii. The intermediate case shows clear interaction between the two parachutes, but without the upper canopy being trapped in the wake of the lower one.

The interaction between two parachutes for various horizontal spacings is further clarified when we

look at the aerodynamic forces acting on the individual canopies. Figure 2 shows the time-averaged drag (D) for the lower and upper canopies for spacings ranging from 0.0 to 5.0. The forces shown in these figures are scaled from the computed values according to the C-9 physical dimensions, the prescribed descent velocity, and the density of air. These scalings differ from the scaling that was initially presented.⁸ The values for the upper canopy drag are fit to a curve using cubic spline and assuming that the curve a) is symmetric at zero horizontal spacing and b) approaches a constant value as the horizontal spacing is large. The drag for the lower canopy at large horizontal spacings is expected to approach the same value of drag as for the upper parachute. This figure shows that the average drag on the upper parachute can become negative for severe interactions between the parachutes, such as for a spacing of 0.5. In these cases, the parachute would risk collapsing. For the intermediate case (i.e., 2.0 radii), the drag on the upper canopy remains positive. However, in this case there is a clear interaction between the two parachutes which could possibly lead to severe structural responses in the fluid-structure interactions of the upper parachute. For 5.0 radii, minimal interaction is seen in the drag history plots.

Figure 3 shows the time-averaged values for the horizontal force component, F_x . For cases in which there is no interaction between the two canopies, the average value of F_x is expected to be zero. For small horizontal spacing (i.e., less than 3.0 radii), the horizontal forces acting on the two canopies are attractive. For the spacings greater than 3.0 radii, the interaction becomes less evident and the difference between F_x for the upper and lower canopies begins to decay. For these larger spacings, carrying the computations further is expected to bring the averaged values of F_x to approximately zero.

As indicated, results from these simulations are useful in understanding when aerodynamic interaction between multiple parachutes is significant. However, sophisticated models are required to better understand the full interaction between parachutes in these cases. Follow-on simulations are being carried out to study the structural response in these cases of significant interaction. Simulations involving relative motions between the two parachutes or structural displacements in the canopy require a special finite element formulation which can handle problems in which the spatial domain occupied by the air is changing in time. For these cases, we use the Deforming-Spatial-Domain/Stabilized Space-Time (DSD/SST) formulation.^{9,10} The DSD/SST formu-

lation, along with an appropriate mesh-update strategy, allows us to study these interaction problems along with either rigid-body motions (for example, from a 6-dof model) or FSI deformations for the parachute structure. These follow-on studies will address some of the more challenging interaction issues, such as parachute canopy collapse.

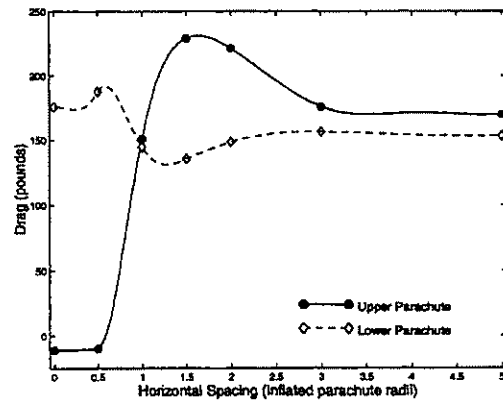


Figure 2. Influence of horizontal spacing on drag, D .

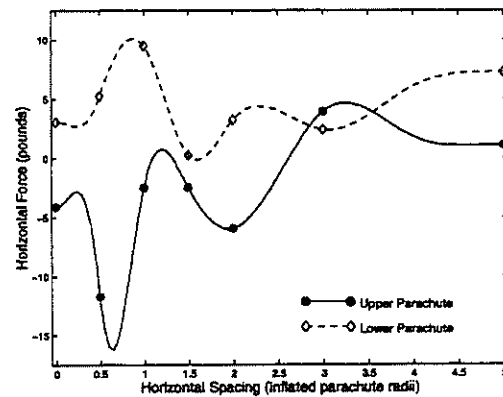


Figure 3. Influence of horizontal spacing on F_x .

Interactions in Parachute Clusters

A series of simulations are carried out for the interaction between the canopies in a cluster of parachutes for three to six canopies. For the cluster simulations, the parachute model is represented by a set of identical C-9 canopies that are positioned and oriented relative to a prescribed confluence point. Two types of configurations are prescribed. First, 3-, 4-, and 6-canopy clusters are defined with the canopies uniformly distributed at a prescribed angle about the azimuthal axis. Secondly, 4-, 5-, and

5-canopy clusters are defined with a single canopy in the center, and the remaining canopies are distributed uniformly at a prescribed angle about the azimuthal axis. The size of the volume mesh varies from case to case, with approximately 2.5 million tetrahedral elements and 450,000 nodes, and resulting in approximately 1.9 million coupled equations for the 5-canopy cluster with a parachute in the center. Mesh refinement is controlled surrounding the canopies and the wake and interaction regions. As with the previous example, descent velocities of 22.0 ft/s are represented by imposing a uniform upstream boundary condition on the lower boundary and no-slip conditions on each of the canopy surfaces.

The computed flow field from these preliminary simulations are shown in Figure 5, depicting the magnitude of the vorticity in two cutting planes for each configuration. The figure shows the vorticity in the $x = 0$ plane (left) and the $y = 0$ plane (right). The center figure shows the arrangement of the canopies in the cluster, as viewed from $z = -\infty$. These initial simulations demonstrate the interactions between canopies in different cluster arrangements.

Further analysis is needed to better understand the other effects influencing the interactions in clusters, such as the preferred arrangements for the canopies, blockage effects due to the finite computational domain, and ultimately fluid-structure interaction effects. For the examples presented, blockage effects are evident and increase with the number of canopies in the cluster. Experimental studies have been conducted to provide empirical correction factors for blockage effects.¹¹ However, these data are dependent on the type of parachute, fluid-structure interactions, and other factors. Additional simulations are being carried out to numerically obtain correction factors for the cases studied.

Additionally, the examples presented neglect the structural response between the canopies in the clusters. The DSD/SST method is being used to study the dynamical interactions between the canopies in the cluster, treating the individual canopies as rigid bodies. Numerical simulations¹² have been conducted previously to predict the equilibrium configuration for clusters of three half-scale C-9 parachutes in comparison with experimental data.¹³ In these simulations, equilibrium configurations were determined using a quasi-static approach and imposing a symmetry configuration for the three canopies. The DSD/SST formulation, along with an appropriate mesh-update strategy, allows us to study the interaction of canopies in a cluster in a dynamic fashion.

Follow-on simulations will be carried out to predict equilibrium configurations for the 3-canopy cluster with and without an imposed symmetry. Additional simulations will be carried out to study the interactions for the 4-, 5-, and 6-canopy clusters. Initially, these studies will treat the canopies as rigid bodies, with later simulations including FSI effects.

CONCLUDING REMARKS

Numerical simulations have been carried out for the aerodynamic interactions between multiple parachute canopies. Interactions between two separate parachutes show significant interactions for horizontal spacings of less than two canopy radii, which could possibly lead to canopy collapse. Preliminary simulations for the interactions between the canopies in a clustered parachute system have also been carried out for 3-6 canopies and for a variety of cluster arrangements.

These simulations provide initial results on the aerodynamic interactions between multiple parachutes and demonstrate the utility of the modeling tools for studies in airdrop applications. These simulations also provide a better understanding of the interactions between multiple parachute canopies and help identify the scenarios under which the interactions are most severe. In the cases of severe interactions, sophisticated fluid-structure interaction models are required to accurately represent the response of the parachute structure.

ACKNOWLEDGEMENT

The work reported in this paper was partially sponsored by NASA JSC (grant no. NAG9-1059), AFOSR (contract no. F49620-98-1-0214), and by the Natick Soldier Center (contract no. DAAD16-00-C-9222). The content does not necessarily reflect the position or the policy of the government, and no official endorsement should be inferred.

References

- [1] C.W. Peterson, J.H. Strickland and H. Higuchi, "The Fluid Dynamics of Parachute Inflation", *Annual Review of Fluid Mechanics*, 28 (1996) 361-387.
- [2] R.J. Benney and K.R. Stein, "A Computational Fluid Structure Interaction Model for Parachute Inflation", *Journal of Aircraft*, 33 (1996) 730-736.

- [3] K.R. Stein, R.J. Benney, V. Kalro, A.A. Johnson and T.E. Tezduyar, "Parallel Computation of Parachute Fluid-Structure Interactions", *Proceedings of the 14th AIAA Aerodynamic Decelerator Systems Technology Conference*, San Francisco, 1997.
- [4] K. Stein, R. Benney, V. Kalro, T. Tezduyar, J. Leonard, and M. Accorsi, "3-D Computation of Parachute Fluid-Structure Interactions: Performance and Control", *Proceedings of the CEAS/AIAA 15th Aerodynamic Decelerator Systems Technology Conference*, AIAA-99-1714, Toulouse, France, 1999.
- [5] C. Ibos, C. Lacroix, A. Goy, and P. Bordenave, "Fluid-Structure Simulation of 3D Ram Air Parachute with Sinpa Software", *Proceedings of the CEAS/AIAA 15th Aerodynamic Decelerator Systems Technology Conference*, AIAA-99-1713, Toulouse, France, 1999.
- [6] T.E. Tezduyar, "Stabilized Finite Element Formulations for Incompressible Flow Computations", *Advances in Applied Mechanics*, **28** (1991) 1-44.
- [7] T.E. Tezduyar and Y. Osawa, "Methods for parallel computation of complex flow problems", *Parallel Computing*, **25** (1999) 2039-2066.
- [8] K. Stein, R. Benney, T. Tezduyar, V. Kumar, E. Thornburg, C. Kyle, and T. Nonoshita, "Aerodynamic Interaction Between Multiple Parachute Canopies", To appear in the *Proceedings of the 1st M.I.T. Conference on Computational Fluid and Structural Mechanics*, Cambridge, Massachusetts, 2001.
- [9] T.E. Tezduyar, M. Behr, and J. Liou, "A new strategy for finite element computations involving moving boundaries and interfaces - the deforming-spatial-domain/space-time procedure: I. The concept and the preliminary tests", *Computer Methods in Applied Mechanics and Engineering*, **94** (1992) 339-351.
- [10] T.E. Tezduyar, M. Behr, S. Mittal, and J. Liou, "A new strategy for finite element computations involving moving boundaries and interfaces - the deforming-spatial-domain/space-time procedure: II. Computation of free-surface flows, two-liquid flows, and flows with drifting cylinders", *Computer Methods in Applied Mechanics and Engineering*, **94** (1992) 353-371.
- [11] J.M. Macha and R.J. Buffington, "Wall-Interference Corrections for Parachutes in a Closed Wind Tunnel", *Proceedings of the AIAA 10th Aerodynamic Decelerator Technology Conference*, AIAA-89-0900, San Diego, 1989.
- [12] J. Sahu and R. Benney, "Prediction of Terminal Descent Characteristics of Parachute Clusters Using CFD", *Proceedings of the AIAA 14th Aerodynamic Decelerator Systems Technology Conference*, AIAA-97-1453, Clearwater Beach, 1997.
- [13] C.K. Lee, J. Lanza, and J. Buckley, "Apparatus and Method for Measuring Angular Positions of Parachute Canopies", *Journal of Aircraft*, **33** (1996) 1197-1199.

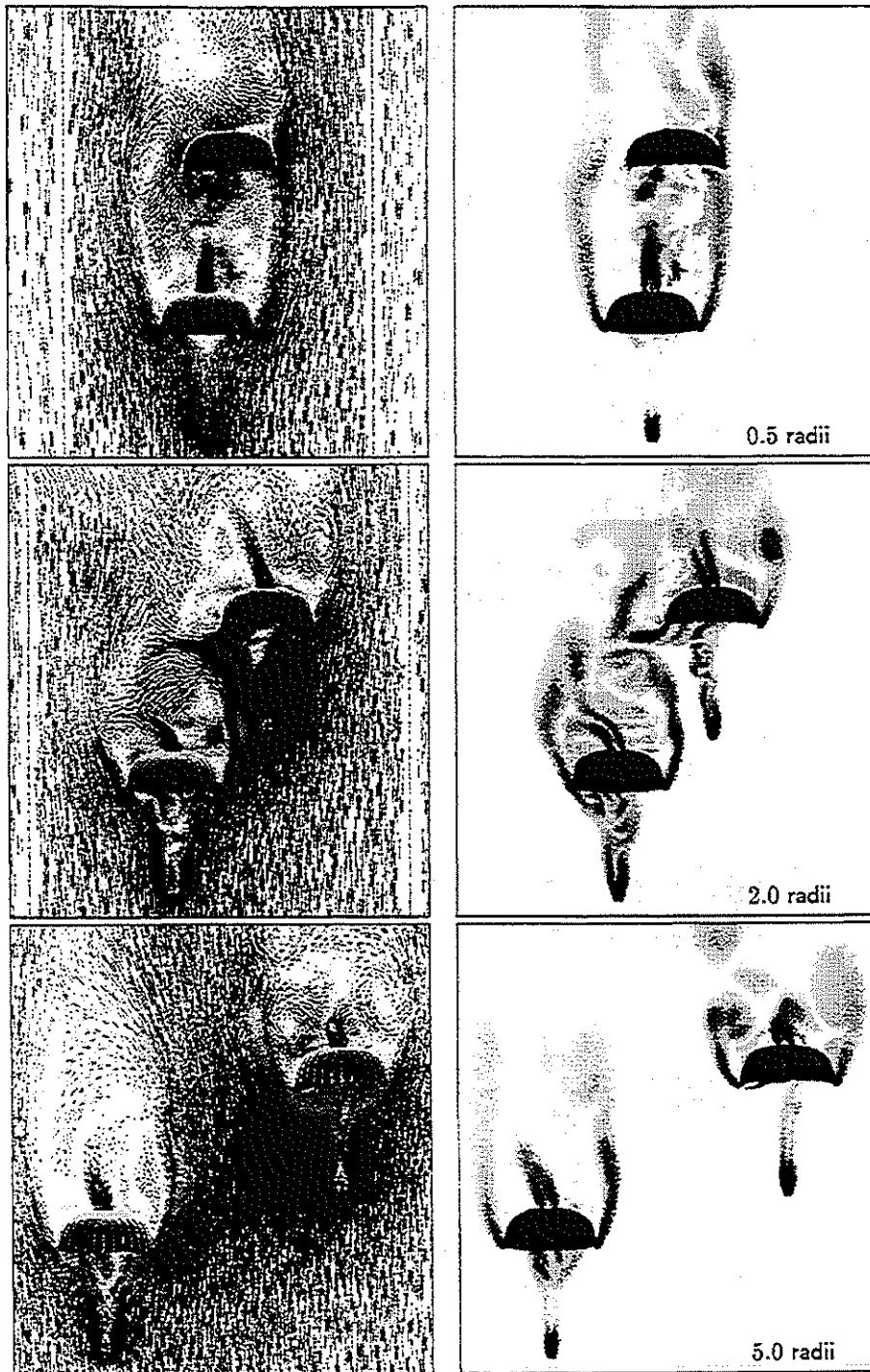


Figure 4. Flow fields for the interaction between two parachutes: Velocity vectors (left); Vorticity (right).

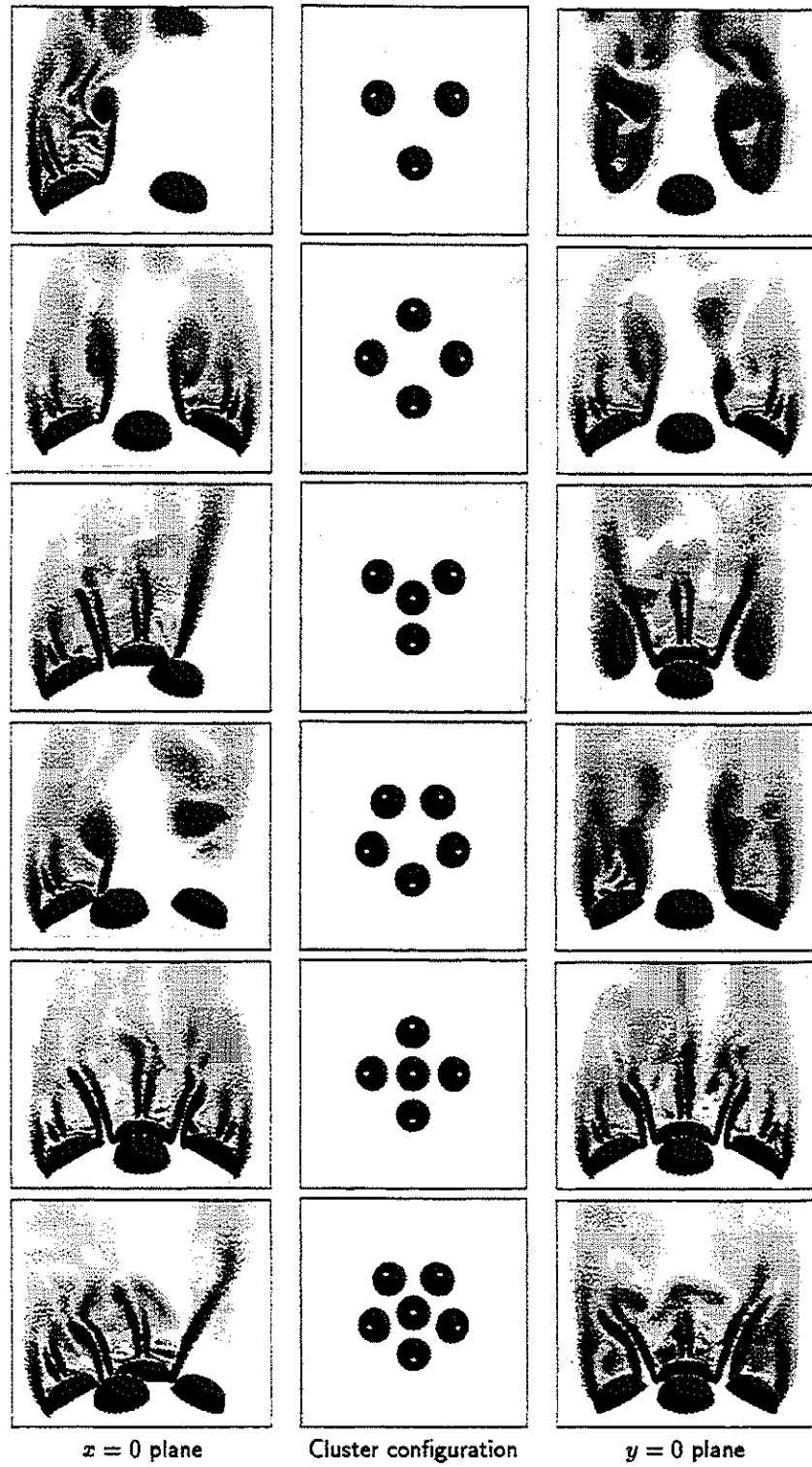


Figure 5. Interaction between canopies in a cluster of parachutes: Vorticity.